Oxygen Molecule Activation on Single-Atom Catalysts with Cu, Ag, and Au: A Cluster Model Study

Yangliu Wu[1,2], Xunlei Ding[1,2*], Wei Li[1,2*], Joseph Israel Gurti[1,2]

[1]School of Mathematics and Physics, North China Electric Power University, Beijing, China
[2]Institute of Clusters and Low Dimensional Nanomaterials, North China Electric Power University, Beijing, China
Email: *dingxl@ncepu.edu.cn, *weil@ncepu.edu.cn

Abstract

$MSi_nO_{2n+1}^-$ (M = Au, Ag, Cu; n = 1, 2, 3) clusters were used as a cluster model to study the activation of oxygen molecules on single-atom catalysts. Structures of $MSi_nO_{2n+1}^-$ clusters were studied by density functional calculations with global optimization. For each n, the most stable structures are quite similar for different metal types, and the oxygen molecule prefers to be adsorbed onto M atoms. It is found that the activation degree of oxygen is higher on clusters with non-noble metal Cu than that of Ag or Au containing clusters, by comparing the changes of O-O bond length and vibrational frequency, natural charge population analysis, Fuzzy bond order analysis, and energy barriers of O_2 dissociation. CO oxidation was used as a probe reaction to study the reactivity of Cu-containing clusters, and it is found that the reactivity decreases with the increase of the size of silicon-oxygen clusters. Our results give a new aspect to understand the reaction mechanism of non-precious metal single-atom catalyst for oxygen activation with high efficiency.

Keywords

Oxygen Activation, Single-Atom Catalysis, Non-Noble Metals, Density Function Theory, Micro-Mechanism

1. Introduction

Oxidation reaction has traditionally been a hot topic in chemistry [1] [2] [3] [4] [5], in which the selection of a proper oxidant is of great importance [6] [7]. In recent years, with the development of the concept of green chemistry, people are more inclined to seek environmentally friendly, cheap, and efficient oxidants [8]

[9] [10] [11]. Molecular oxygen (O_2), the environmentally friendly oxidizing agent is undoubtedly attractive, which is highly valued by chemists because of its cheapness [12] [13] [14], easy availability, and non-pollution of the product to the environment. However, O_2 is quite stable at room temperature due to the tightly bound O-O bond. So it is a key step to select a suitable catalyst to activate O_2 and open the O-O bond. There are many ways to activate oxygen. One of the effective ways is the combination of oxygen molecules with transition metal compounds. As electrons transfer from the metal center to the oxygen molecule, the bond length of O-O bond becomes longer and the oxygen molecule activates. Many research groups have studied the mechanism of it. Safonova and co-workers [15] studied the oxygen activation mechanism on ceria-supported copper-oxo species using time-resolved X-ray absorption spectroscopy. It was found that in this system oxygen activation involves copper-oxo species in close interaction with ceria. Laura and co-workers [16] compared oxygen activation catalyzed by pure gold cluster Au_{13} and $Au_{12}M$ (M = Ag, Cu, Ir) cluster, respectively. It found that the activation energy barrier for the O_2 dissociation of $Au_{12}M$ cluster is lower nearly 1 eV than that of Au_{13} cluster. Manzoor and Pal [17] made hydrogen atom chemisorption on the stable closed-shell gold clusters neutral Au_n (n = 2, 4, 6, 8) gold clusters with DFT calculations then catalyst oxygen with Au_nH clusters. The enhanced binding energies and significant red shift in the O-O stretching frequency unequivocally confirm the activation of the O_2 molecule in the case of Au_nH clusters.

A new idea has been developed for catalyst design since Zhang *et al.* who proposed the concept of single-atom catalysts (SACs) in their work in 2011 [18]. Because the active center in single-atom catalysts only contains a single metal atom, the atomic utilization of precious metals has been raised to the limitation. Since then, SACs have been an important subject of research in the catalysis field [19]. Due to the complexity of actual catalysts, there are still many unrevealed mechanisms in surface catalytic reactions even for SAC systems. Clusters of finite atoms are easy to deal with experimentally and computationally, the study of reasonable cluster models can be used as a bottom-up strategy to understand complex systems and processes [20] [21]. The structure of single-atom catalysts is uniform, and the cluster composed of active single atom and several surrounding atoms can be used as a reasonable model to study the reaction mechanisms.

In the previous work of our group [22], we found that $AuSi_nO_{2n+1}^-$ (n = 1, 2, 3) clusters perform well in the catalytic activation of methane. In order to further study the reactivity of $AuSi_nO_{2n+1}^-$ and explore the possibility of replacing Au with non-precious metals, we performed a systematical investigation on $MSi_nO_{2n+1}^-$, which M could be Au, Ag, and Cu. For all the Cu-group metals, the outermost electron configuration is the same: a closed outermost d-shell and a single s-valence electron. Therefore, Cu, a non-precious element, containing clusters may exhibit similar properties to clusters with gold atoms [23].

In this paper, we report the most stable structures of $MSi_nO_{2n+1}^-$ clusters (M = Au, Ag, and Cu; n = 1, 2, 3) calculated by density functional theory (DFT). Based on that, the adsorption and dissociation of O_2 on the clusters are discussed. It was found that Cu-containing clusters performed better than Au- or Ag-containing clusters. Therefore, further calculations on CO oxidation, which is used as a probe reaction, are only performed on Cu-containing clusters.

2. Calculation Method

All our DFT calculations were performed using Gaussian 09 program suite [24]. A Fortran code [25] based on a genetic algorithm and DFT calculations was developed to generate sufficient and reasonable initial structures of $MSi_nO_{2n+1}^-$ clusters, which have also been successfully applied to some other clusters [26]-[31]. TZVP basis sets [32] for C, O, and Si atoms and the D95V basis sets combined with the Stuttgart/Dresden relativistic effective core potentials (denoted as SDD in Gaussian software) for Au atom were adopted [33]. Diffusion functions are essential for anionic clusters. Therefore, we modified the original TZVP and SDD basis sets with additional diffusion functions according to the approach proposed by Truhlar *et al.* [34] [35]. In this approach, the smallest exponents of s and p functions in the original basis sets are divided by 3 and then used as the exponent of the additional diffusion function. TPSS functional [36] was used in this work, since it had been tested to perform well for Au-Si-O systems [22]. Both singlet and triplet states were considered for the oxygen adsorption systems. The spin-crossing points of triplet and singlet states during the oxygen adsorption process were located by utilizing sobMECP software [37]. Natural population analysis (NPA) was carried out using the NBO3.1 module embedded in the Gaussian 09 package. Fuzzy bond order calculations (FBO) were performed using Multiwfn [38] software. Harmonic vibrational frequency calculations were performed on optimized structures at the same theoretical level to ascertain the nature of the stationary points (no imaginary frequencies for minima and only one imaginary frequency for transition states). All results of energy reported in this work are total electronic energy with zero-point vibrational energy (ZPE) correction unless specified.

3. Results and Discussion

3.1 The Most Stable Structures of $MSi_nO_{2n+1}^-$ Clusters

The calculated most stable structures of $MSi_nO_{2n+1}^-$ clusters are presented in Figure 1. Clusters with three kinds of metal atoms (Au, Ag, Cu) have similar geometric structures and the same electronic states, except for the slight differences in bond lengths and bond angles. All the $MSiO_3^-$ and $MSi_2O_5^-$ clusters have C_{2V} symmetry and $^1A_1$ electronic state, while $MSiO_3^-$ clusters have C_1 symmetry and ^1A electronic state. Details of the M-O bond lengths and M-O-Si bond-angles are shown in Table 1.
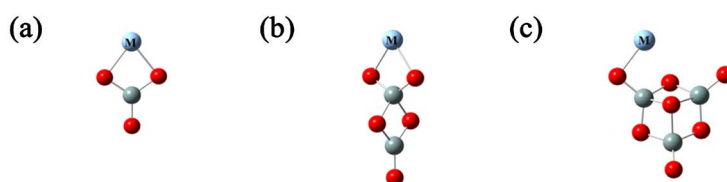
Figure 1. TPSS optimized most stable structures of $MSi_nO_{2n+1}^-$ clusters. (a) $n = 1$; (b) $n = 2$; (c) $n = 3$.

Table 1. Calculated bond lengths and bond angles in $MSi_nO_{2n+1}^-$ clusters.

Clusters	Bond length of M-O (Å)	Bond angle of M-O-Si (°)
$AuSiO_3^-$	2.28	88.15
$AuSi_2O_5^-$	2.30	85.31
$AuSi_3O_7^-$	2.03	107.94
$AgSiO_3^-$	2.25	87.68
$AgSi_2O_5^-$	2.27	85.10
$AgSi_3O_7^-$	2.22	91.30
$CuSiO_3^-$	1.99	83.77
$CuSi_2O_5^-$	2.01	81.53
$CuSi_3O_7^-$	1.95	88.65

3.2. Adsorption of O₂ on $MSi_nO_{2n+1}^-$ Clusters

The most stable adsorption structures of O_2 on optimized $MSi_nO_{2n+1}^-$ clusters are shown in **Figure 2** and some data are listed in **Table 2**. The triplet states of the adsorption structures for each cluster are considered at first, since the ground state of O_2 is a triplet. On Au/Ag-containing clusters, O_2 takes end-on adsorption coordination to the metal atom, while on the Cu-containing clusters, O_2 takes side-on coordination to Cu. After the adsorption, the electronic state may be changed due to spin flip. Therefore, the singlet states are also considered. In all the singlet state structures, O_2 takes side-on coordination on metal atoms. A spin-crossover may occur in the potential energy surfaces of singlet and triplet states when O_2 adsorbs onto the metal atoms in $MSi_nO_{2n+1}^-$. The minimum energy crossing points (MECP) were determined by the sobMECP program combined with the Gaussian 09 package, and the conversion from the triple-state to the singlet state is shown in **Figure 2**. The triplet state is less stable than the singlet state for $n = 1, 2$ clusters, and the conversion from the triplet to the singlet state is quite easy, with low energy barriers (*i.e.*, the relative energy of MECP with respect to the triplet state) as about 0.2 eV for Au-containing clusters and less than 0.1 eV for Ag/Cu-containing clusters. For the relatively larger clusters ($n = 3$), the triplet state is more stable and the conversion from the triplet to the singlet need additional energy, and the
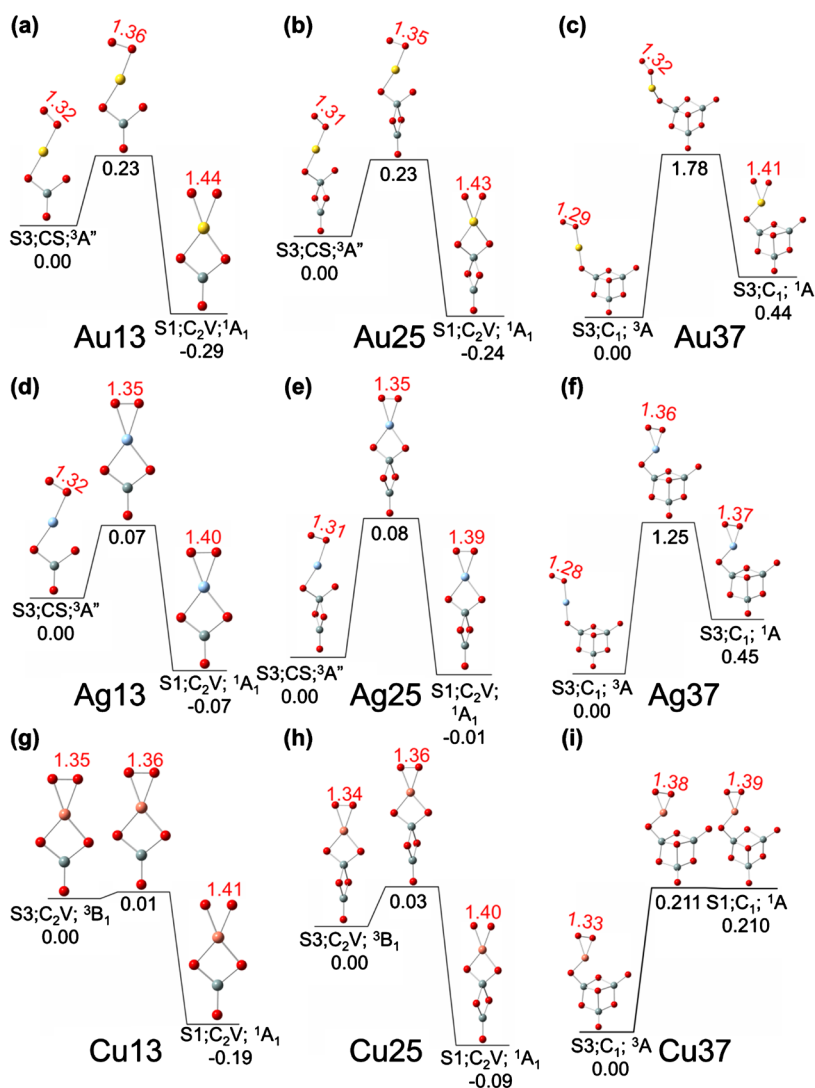
Figure 2. TPSS optimized most stable structures of adsorption complexes $MSi_nO_{2n+1}^-$-O_2, denoted as the label M(n)($2n + 1$), and their spin crossover structures. For (a), (b), (c), M = Au; for (d), (e), (f), M = Ag; for (e), (f), (g), M = Cu. The unit of bond length is Å, and the unit of energy is eV. The left part of each picture is the singlet structure, the right part is the triplet structure, and the middle part is the spin cross-point structure.

barriers of Au/Ag-containing clusters are quite large (1.78 and 1.25 eV, respectively), while that of $CuSi_3O_7^-$ is still small (−0.21 eV). Note that the energies in **Figure 2** are without ZPE corrections since harmonic vibrational frequency calculations can not be performed on MECPs which are not stationary points.

The adsorption energy (E_{ad}) of O_2 on $MSi_nO_{2n+1}^-$ clusters was calculated as $E_{ad} = E(MSi_nO_{2n+1}^-) + E(O_2) - E(MSi_nO_{2n+1}^--O_2)$, where E is the energy of free singlet $MSi_nO_{2n+1}^-$, triplet O_2, and the adsorption complex $MSi_nO_{2n+1}^--O_2$ with either singlet or triplet states, respectively. Four types of energies were considered, namely, E_e (electronic energies), E_{ZPE} (sum of electronic and zero-point energies), E_H (sums of electronic and thermal enthalpies) and E_G (sum of electronic and Gibbs free energies) at the standard temperature (298.15 K) and

Table 2. Properties of the adsorption complexes $MSi_nO_{2n+1}^--O_2$. The adsorption energy (E_e, E_{ZPE}, E_H, and E_G, in eV. See text for details), the vibrational frequency of O-O (v_{O-O}, in cm^{-1}), the S^2 values before and after annihilation. S_1 is for the singlet state, S_3 is for the triplet state.

Clusters	E_e	E_{ZPE}	E_H	E_G	v_{O-O}	S^2 before	S^2 after
$AuSiO_3^--O_2$							
S_1	1.86	1.77	1.82	1.24	920.0	0	0
S_3	1.57	1.51	1.53	1.07	1111.8	2.0081	2
$AuSi_2O_5^--O_2$							
S_1	1.62	1.54	1.57	1.05	929.6	0	0
S_3	1.38	1.32	1.34	0.92	1130.3	2.0083	2
$AuSi_3O_7^--O_2$							
S_1	0.68	0.61	0.64	0.11	967.2	0	0
S_3	1.13	1.10	1.10	0.72	1198.2	2.0075	2
$AgSiO_3^--O_2$							
S_1	1.27	1.20	1.23	0.73	976.5	0	0
S_3	1.20	1.17	1.17	0.81	1137.0	2.0075	2
$AgSi_2O_5^--O_2$							
S_1	0.97	0.90	0.93	0.43	998.4	0	0
S_3	0.97	0.94	0.94	0.58	1156.1	2.0075	2
$AgSi_3O_7^--O_2$							
S_1	0.16	0.11	0.13	-0.38	1138.0	0	0
S_3	0.61	0.59	0.59	0.25	1240.2	2.0076	2
$CuSiO_3^--O_2$							
S_1	2.19	2.11	2.14	1.64	965.12	0	0
S_3	2.00	1.96	1.97	1.55	1088.4	2.0071	2
$CuSi_2O_5^--O_2$							
S_1	1.94	1.85	1.89	1.37	986.1	0	0
S_3	1.85	1.80	1.81	1.40	1100.2	2.007	2
$CuSi_3O_7^--O_2$							
S_1	1.18	1.11	1.13	0.63	1018.9	0	0
S_3	1.38	1.34	1.35	0.92	1138.0	2.0069	2

pressure (1 atm). The results are given in Table 2. Generally, Cu-containing clusters and smaller clusters have higher E_b values than Au/Ag-containing clusters and larger clusters. The values of E_{ZPE} are close to or more than 1 eV for most clusters, indicating that O_2 can be firmly adsorbed on these clusters. $AuSi_3O_7^--O_2$ (S_1) and $AgSi_3O_7^--O_2$ (S_3) have small values for E_{ZPE} as about 0.6

eV, and $AgSi_3O_7^-$-O_2 (S_1) has the smallest E_{ZPE} as 0.11 eV. Because the adsorption of O_2 on clusters leads to the decrease of entropy, the values of E_G are smaller than those of E_{ZPE} by about 0.4 eV. Therefore, $AgSi_3O_7^-$-O_2 (S_1) has a negative value (−0.38 eV) for E_G, indicating that this complex can not be formed at standard conditions.

Vibrational frequencies of O-O (v_{O-O}) in the adsorption complexes $MSi_nO_{2n+1}^-$-O_2 are useful information to evaluate the activation of O_2 after adsorption. The calculated results are shown in Table 2. Upon adsorption, the O-O bond will be weakened, leading to the decrease of v_{O-O} in the adsorption complexes, accompanied by the increase of O-O bond lengths (R_{O-O}). For the triplet state, comparing with Au/Ag-containing clusters, the v_{O-O} of Cu-containing clusters is smaller than those of Au/Ag-containing clusters. Accordingly, the R_{O-O} of Cu-containing clusters is between 1.33 Å and 1.35 Å, which is longer than those of Au/Ag-containing clusters, about 1.28 Å and 1.33 Å. Relatively larger clusters (n = 3) have larger v_{O-O} and shorter R_{O-O} than n = 1, 2 clusters. For example, the v_{O-O} of $AuSi_3O_7^-$ is 1138.0 cm^{-1}, which is 37.8 and 49.6 cm^{-1} larger than $AuSi_2O_5^-$ and $AuSiO_3^-$, respectively, and their R_{O-O} is 1.33, 1.34, and 1.35 Å, respectively. After the transition from triplet to singlet states, the v_{O-O} decreases remarkably and the R_{O-O} increases significantly, indicating high activation of O_2 in the singlet states. For the singlet state, different from the triplet state, the R_{O-O} values of Au-containing clusters are the biggest, which are between 1.41 Å and 1.44 Å, while those of Cu/Ag-containing clusters are between 1.37 Å and 1.41 Å. Accordingly, the v_{O-O} of Au-containing clusters is the smallest. Similar to the situation for triplet states, the v_{O-O} of the relatively larger clusters (n = 3) is larger than that of n = 1, 2 clusters. Note that the calculated S^2 values before and after annihilation indicate that all electronic states we obtained have no spin pollution.

Bond order analysis is a direct way to evaluate the bonding strength between two atoms. We calculated the Fuzzy bond order (FBO) of O-O in the adsorption complexes $MSi_nO_{2n+1}^-$-O_2, and compared with that of free O_2 molecule obtained at the same theoretical level. After adsorption, FBO decreases from 2.47 for free O_2 to values less than 2 for the triplet states. Cu-containing clusters and smaller clusters have lower FBO values than Au/Ag-containing clusters and larger clusters, which is consistent with the conclusion that Cu-containing clusters and smaller clusters have higher ability to activate O_2 according to the analysis basis on R_{O-O} and v_{O-O}. After the transition from triplet to singlet states, FBO decrease to low values about 1.4, indicating that O-O in the singlet $MSi_nO_{2n+1}^-$-O_2 is highly activated, which is consistent with the long R_{O-O} and small v_{O-O} for them.

The activation of O-O bonds in the adsorption complexes $MSi_nO_{2n+1}^-$-O_2 can also be reflected by the electron transfer from $MSi_nO_{2n+1}^-$ to O_2. The O_2 molecule obtains electrons after adsorption and these electrons will fill into the π^* anti-bonds of O-O, leading to the weakening of O-O bond. Natural population analysis (NPA) was performed to get the charges on O_2 (q_{O_2}), and the results are shown in Figure 4. It is clear that q_{O_2} of the triplet states is smaller (for absolute
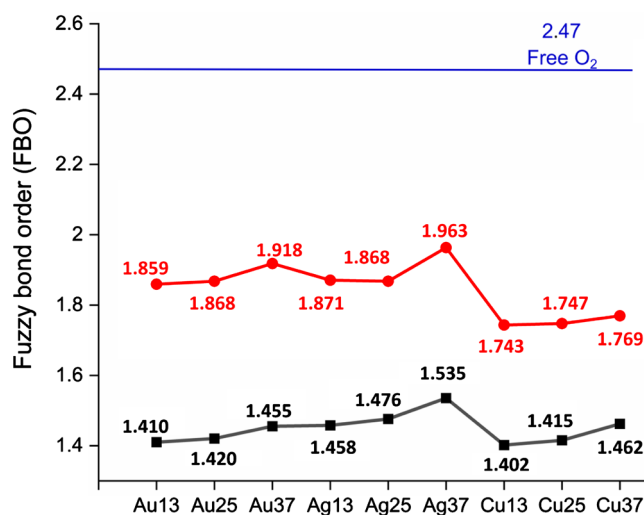
Figure 3. Fuzzy bond order (FBO) of O_2 in the adsorption complexes $MSi_nO_{2n+1}^- -O_2$ (denoted as the label $M(n)(2n+1)$). The red line represents the triplet state, the black line represents the singlet state, and the blue line represents the FBO value of free oxygen.
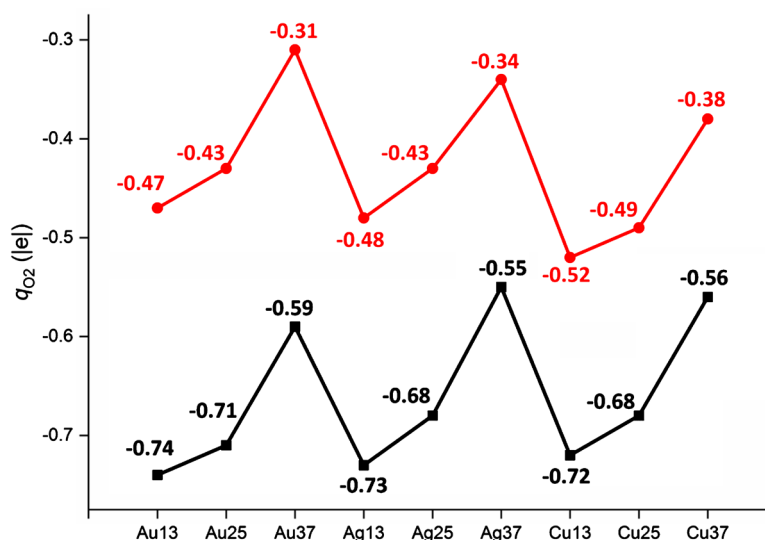

Figure 4. Natural population analysis (NPA) charge on O_2 in the adsorption complexes $MSi_nO_{2n+1}^- -O_2$ (denoted as the label $M(n)(2n+1)$). The red line represents the triplet state, the black line represents the singlet state.

values) than that of the singlets. The oscillation of the curve shows that for each case (a certain metal and a certain electronic state), q_{O_2} decreases as n increases from 1 to 3. For the triplet state, Cu-containing clusters have larger q_{O_2} than Au/Ag-containing clusters with the same cluster sizes, while for the singlet state, q_{O_2} of Au-containing clusters is the largest for each n. All these findings agree well with the previous discussion on the activation of O_2 based on R_{O-O}, v_{O-O}, and FBO.

3.3 Reactions of $CuSi_nO_{2n+1}^- -O_2$ with CO

Oxidation of CO is often used as a probe reaction to evaluate the oxidation abil-

ity of oxidants. Considering the high energy barriers of spin flip from the triplet state to singlet state for the adsorption complexes $AuSi_nO_{2n+1}^--O_2$ and $AgSi_nO_{2n+1}^--O_2$, a systematical study was performed on the oxidation of CO on Cu-containing clusters, which may be the most promising catalysts for CO oxidation. Because the ground states of $CuSiO_3^-$ and $CuSi_2O_5^-$ are the singlet state and the ground state of $CuSi_3O_7^-$ clusters is the triplet state, both singlet and triplet states along the reaction paths were calculated. The sum of the energy of infinite separated CO and the ground state of $CuSi_nO_{2n+1}^--O_2$ was set to zero. **Figure 5(a)** shows the reaction path of $CuSiO_3^--O_2$ (IS1) with CO. It can be started from the singlet $^1IS1$ with CO, because $^1IS1$ is lower in energy than $^3IS1$ by 0.155 eV, and the transition from $^3IS1$ to $^1IS1$ is very easy (the energy barrier is only 0.01 eV, **Figure 2**). The CO is then weakly adsorbed on an O atom to form $^1I1$ with a low adsorption energy −0.066 eV. The distance between the C and the O in $^1IS1$ ($d_{C\cdots O}$) is quite far (2.724 Å) at this moment. Then the CO moves much more close to the cluster and climbs over a transition state ($^1TS1$), whose overall relative energy is as high as 0.747 eV and $d_{C\cdots O}$ in $^1TS1$ is 1.540 Å. After the transition state, a CO_2 moiety is formed as in $^1I2$ which is very stable with a low relative energy (−2.739 eV). In the last step, the system desorbs a CO_2, forming $^3CuSiO_4^-$ (−2.119 eV) through a spin-crossover, or $^1CuSiO_4^-$ (−1.744 eV). The whole path of the singlet stats is below that of the triplet, except the products, indicating that the singlet states are preferred for $CuSiO_3^--O_2$ (IS1) with CO. Similarly situations are found for the reaction of $CuSi_2O_5^--O_2$ (IS2) with CO, as shown in **Figure 5(b)**. Differently, the reaction path of $CuSi_3O_7^--O_2$ (IS3) with CO prefers triplet states (**Figure 5(c)**). Consistent with the previous discussion, the smallest system $CuSiO_3^--O_2$ has the lowest energy barrier and therefore the highest oxidation ability toward CO. These three paths are compared with our previous work in which $AuVO_{1,2}^+$ were used to catalyse the reaction of CO to CO_2 by O_2. [39] The difference between the two works is CO attack site. In our work, CO prefers O site of the activated oxygen, while CO prefers mental site in $AuVO_{1,2}^+$ system. Rate-determining step (RDS) barrier means a lot when study reaction. The RDS barrier of previous work is from 1.100 eV to 2.470 eV, while that is from 0.817 eV to 0.992 eV in this work.

4. Conclusion

The geometric and electronic properties of anionic $MSi_nO_{2n+1}^-$ (M = Au, Ag, Cu; *n* = 1, 2, 3) clusters for the most stable structures, together with the adsorption and dissociation of O_2 molecule on them, were systematically studied by DFT calculations. For the triplet state, O_2 takes two kinds of adsorption coordination to the metal atom, end-on adsorption coordination for Au/Ag-containing clusters, and side-on coordination for Cu-containing. The adsorbed O_2 may be further activated by changing into singlet states, for which O_2 takes side-on coordination on metal atoms. The barriers for the transition from the triplet states to the singlet states, obtained by MECP calculations, are quite larger for
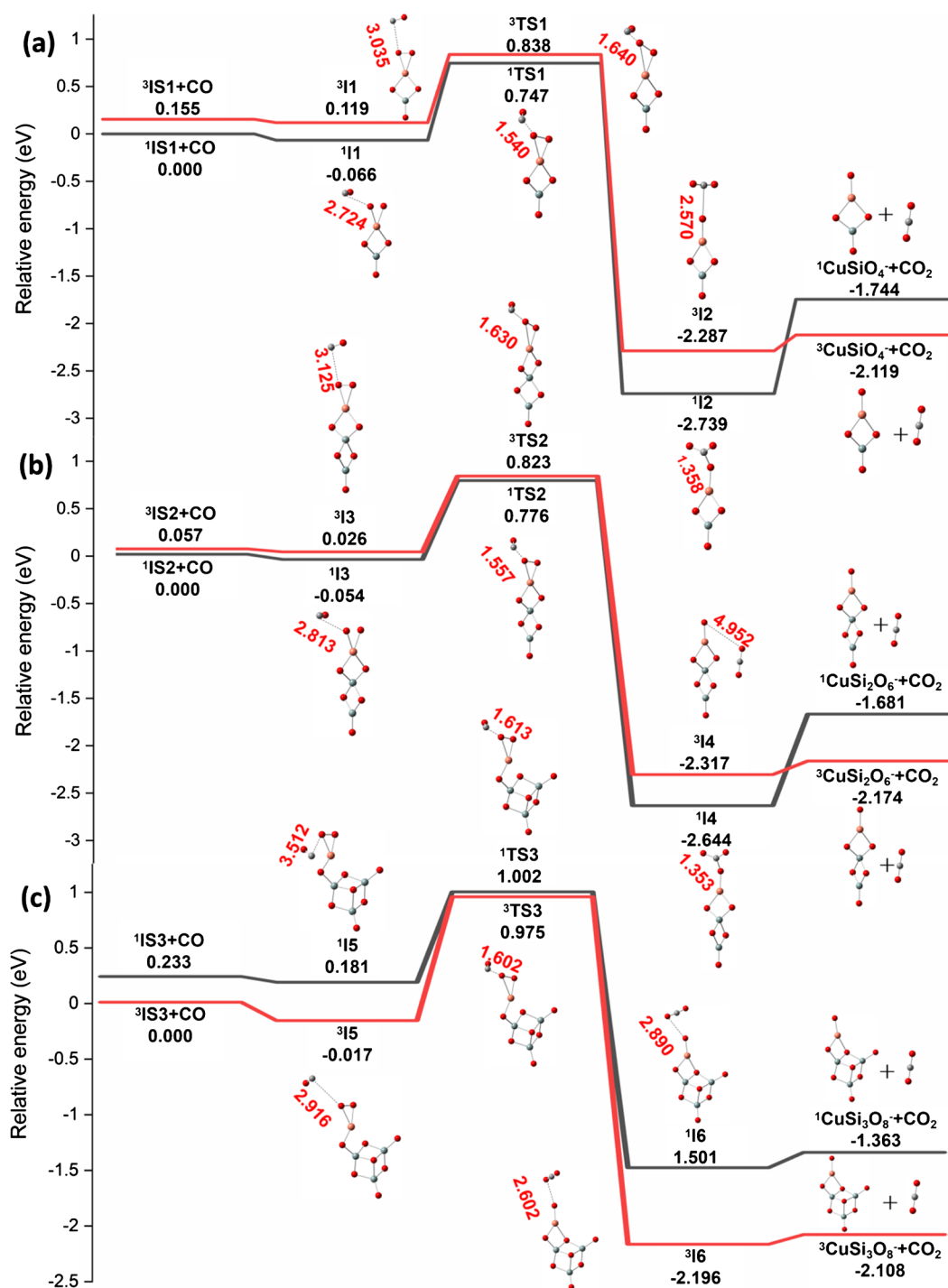
Figure 5. DFT calculated potential energy profiles for $CuSi_nO_{2n+1}^- \text{-} O_2$ clusters desorb CO_2 after reacting with CO. IS1: $CuSiO_3^- \text{-} O_2$; IS2: $CuSi_2O_5^- \text{-} O_2$; IS3: $CuSi_3O_7^- \text{-} O_2$.

Au/Ag-containing clusters than for Cu-containing clusters. By comparing the bond length, the vibrational frequency, FBO, and NPA charge on the adsorbed O_2 moiety, it is found that smaller clusters always have higher reactivity toward O_2, and Cu-containing clusters can absorb and activate oxygen in a higher degree than Au/Ag-containing clusters for the triplet states. Although Au-containing

clusters are more active toward O_2 than Cu/Ag-containing clusters for the singlet states, the transitions from the triplet states to the singlet states for $AuSi_nO_{2n+1}^- \text{-} O_2$ all have relatively high barriers. CO oxidation was used as a probe reaction to study the reactivity of Cu-containing clusters and confirmed that the reactivity decreases with the increase of the size of $CuSi_nO_{2n+1}^-$ clusters. Our results may provide a useful guide for the rational design of non-noble metal SACs for oxygen activation based on Cu-containing materials at the molecular level.

Acknowledgements

Conflicts of Interest

The authors declare no conflicts of interest regarding the publication of this paper.

References

[1] Nematollahi, P. and Neyts, E.C. (2018) A Comparative DFT Study on CO Oxidation Reaction over Si-Doped BC_2N Nanosheet and Nanotube. *Applied Surface Science*, **439**, 934-945. https://doi.org/10.1016/j.apsusc.2017.12.254

[2] Tang, Y.A., Chen, W.G., Shen, Z.G., Li, C.G., Ma, D.W. and Dai, X.Q. (2018) A Computational Study of CO Oxidation Reactions on Metal Impurities in Graphene Divacancies. *Physical Chemistry Chemical Physics*, **20**, 2284-2295. https://doi.org/10.1039/C7CP07397F

[3] Esrafili, M.D., Nematollahi, P. and Abdollahpour, H. (2016) A Comparative DFT Study on the CO Oxidation Reaction over Al- and Ge-Graphene as Efficient Metal-Free Catalysts. *Applied Surface Science*, **378**, 418-425. https://doi.org/10.1016/j.apsusc.2016.04.012

[4] Fu, Q., Yang, F. and Bao, X. (2013) Interface-Confined Oxide Nanostructures for Catalytic Oxidation Reactions. *Accounts of Chemical Research*, **46**, 1692-1701. https://doi.org/10.1021/ar300249b

[5] Xie, Y., Dong, F. and Bernstein, E.R. (2011) Experimental and Theory Studies of the Oxidation Reaction of Neutral Gold Carbonyl Clusters in the Gas Phase. *Catalysis Today*, **177**, 64-71. https://doi.org/10.1016/j.cattod.2011.01.047

[6] Zhu, Q., Wegener, S.L., Xie, C., Uche, O., Neurock, M. and Marks, T.J. (2013) Sulfur as a Selective "Soft" Oxidant for Catalytic Methane Conversion Probed by Experiment and Theory. *Nature Chemistry*, **5**, 104-109. https://doi.org/10.1038/nchem.1527

[7] Kurten, T., Lane, J.R., Jorgensen, S. and Kjaergaard, H.G. (2011) A Computational Study of the Oxidation of SO_2 to SO_3 by Gas-Phase Organic Oxidants. *The Journal of Physical Chemistry A*, **115**, 8669-8681. https://doi.org/10.1021/jp203907d

[8] Sharma, P.K., de Visser, S.P., Ogliaro, F. and Shaik, S. (2003) Is the Ruthenium Analogue of Compound I of Cytochrome P450 an Efficient Oxidant? A Theoretical Investigation of the Methane Hydroxylation Reaction. *Journal of the American Chemical Society*, **125**, 2291-2300. https://doi.org/10.1021/ja0282487

[9] Angelika, W.R., Bialecka, B. and Thomas, M. (2020) Application of Calcium Perox-

ide as an Environmentally Friendly Oxidant to Reduce Pathogens in Organic Fertilizers and Its Impact on Phosphorus Bioavailability. *Archives of Environmental Protection*, **46**, 42-53.

[10] Peckh, K., Lisicki, D., Talik, G. and Orlińska, B. (2020) Oxidation of Long-Chain α-Olefins Using Environmentally-Friendly Oxidants. *Materials*, **13**, 4545. https://doi.org/10.3390/ma13204545

[11] Ottenbacher, R.V., Talsi, E.P. and Bryliakov, K.P. (2020) Recent Progress in Catalytic Oxygenation of Aromatic C-H Groups with the Environmentally Benign Oxidants H_2O_2 and O_2. *Applied Organometallic Chemistry*, **34**, e5900. https://doi.org/10.1002/aoc.5900

[12] Jia, M.Y., Luo, Z.X., He, S.G. and Ge, M.F. (2014) Oxygen-Sulfur Exchange and the Gas-Phase Reactivity of Cobalt Sulfide Cluster Anions with Molecular Oxygen. *The Journal of Physical Chemistry A*, **118**, 8163-8169. https://doi.org/10.1021/jp500837g

[13] Ding, X.L., Li, Z.Y., Yang, J.L., Hou, J.G. and Zhu, Q.S. (2004) Adsorption Energies of Molecular Oxygen on Au Clusters. *The Journal of Chemical Physics*, **120**, 9594-9600. https://doi.org/10.1063/1.1665323

[14] Xiao, M.L., Zhu, J.B., Li, G.R., Li, N., Li, S., Cano, Z.P., Ma, L., Cui, P.X., Xu, P., Jiang, G.P., Jin, H.L., Wang, S., Wu, T.P., Lu, J., Yu, A.P., Su, D. and Chen, Z.W. (2019) A Single-Atom Iridium Heterogeneous Catalyst in Oxygen Reduction Reaction. *Angewandte Chemie International Edition*, **58**, 9640-9645. https://doi.org/10.1002/anie.201905241

[15] Safonova, O.V., Guda, A., Rusalev, Y., Kopelent, R., Smolentsev, G., Teoh, W.Y., van Bokhoven, J.A. and Nachtegaal, M. (2020) Elucidating the Oxygen Activation Mechanism on Ceria-Supported Copper-Oxo Species Using Time-Resolved X-Ray Absorption Spectroscopy. *ACS Catalysis*, **10**, 4692-4701. https://doi.org/10.1021/acscatal.0c00551

[16] Jiménez-Díaz, L.M. and Pérez, L.A. (2018) Molecular Oxygen Adsorption and Dissociation on $Au_{12}M$ Clusters with M = Cu, Ag or Ir. *The European Physical Journal D*, **72**, 51. https://doi.org/10.1140/epjd/e2018-80508-2

[17] Manzoor, D. and Pal, S. (2014) Hydrogen Atom Chemisorbed Gold Clusters as Highly Active Catalysts for Oxygen Activation and CO Oxidation. *The Journal of Physical Chemistry C*, **118**, 30057-30062. https://doi.org/10.1021/jp510488v

[18] Qiao, B.T., Wang, A.Q., Yang, X.F., Allard, L.F., Jiang, Z., Cui, Y.T., Liu, J.Y., Li, J. and Zhang, T. (2011) Single-Atom Catalysis of CO Oxidation Using Pt_1/FeO_x. *Nature Chemistry*, **3**, 634-641. https://doi.org/10.1038/nchem.1095

[19] Jin, Y.Y., Hao, P.P., Ren, J. and Li, Z. (2015) Single Atom Catalysis: Concept, Method and Application. *Progress in Chemistry*, **27**, 1689-1704.

[20] Liu, Q. and He, S. (2014) Oxidation of Carbon Monoxide on Atomic Clusters. *Chemical Journal of Chinese Universities—Chinese*, **35**, 665-688.

[21] Baloglou, A., Oncak, M., Grutza, M.L., van der Linde, C., Kurz, P. and Beyer, M.K. (2019) Structural Properties of Gas Phase Molybdenum Sulfide Clusters $[Mo_3S_{13}]^{2-}$, $[HMo_3S_{13}]^-$, and $[H_3Mo_3S_{13}]^+$ as Model Systems of a Promising Hydrogen Evolution Catalyst. *The Journal of Physical Chemistry C*, **123**, 8177-8186. https://doi.org/10.1021/acs.jpcc.8b08324

[22] Chen, Y.M., Wang, L.N., Chen, J.J., Chen, Q., Jiang, L.X., Zhao, Y.X., Ding, X.L. and He, S.G. (2018) Mechanistic Variants in Methane Activation Mediated by Gold(I) Supported on Silicon Oxide Clusters. *Chemistry—A European Journal*, **24**, 17506-17512. https://doi.org/10.1002/chem.201803432

[23] Hirabayashi, S., Ichihashi, M., Kawazoe, Y. and Kondow, T. (2012) Comparison of Adsorption Probabilities of O_2 and CO on Copper Cluster Cations and Anions. *The Journal of Physical Chemistry A*, **116**, 8799-8806. https://doi.org/10.1021/jp304214m

[24] Frisch, M.J., Trucks, G.W., Schlegel, H.B., Scuseria, G.E., Robb, M.A., Cheeseman, J.R., Scalmani, G., Barone, V., Petersson, G.A., Nakatsuji, H., Li, X., Caricato, M., Marenich, A.V., Bloino, J., Janesko, B.G., Gomperts, R., Mennucci, B., Hratchian, H.P., Ortiz, J.V., Izmaylov, A.F., Sonnenberg, J.L., Williams, Ding, F., Lipparini, F., Egidi, F., Goings, J., Peng, B., Petrone, A., Henderson, T., Ranasinghe, D., Zakrzewski, V.G., Gao, J., Rega, N., Zheng, G., Liang, W., Hada, M., Ehara, M., Toyota, K., Fukuda, R., Hasegawa, J., Ishida, M., Nakajima, T., Honda, Y., Kitao, O., Nakai, H., Vreven, T., Throssell, K., Montgomery, J.A., Peralta, J.E., Ogliaro, F., Bearpark, M.J., Heyd, J.J., Brothers, E.N., Kudin, K.N., Staroverov, V.N., Keith, T.A., Kobayashi, R., Normand, J., Raghavachari, K., Rendell, A.P., Burant, J.C., Iyengar, S.S., Tomasi, J., Cossi, M., Millam, J.M., Klene, M., Adamo, C., Cammi, R., Ochterski, J.W., Martin, R.L., Morokuma, K., Farkas, O., Foresman, J.B. and Fox, D.J. (2016) Gaussian 09 Rev. D.01. Gaussian Inc., Wallingford.

[25] Ding, X.L., Li, Z.Y., Meng, J.H., Zhao, Y.X. and He, S.G. (2012) Density-Functional Global Optimization of $(La_2O_3)_n$ Clusters. *The Journal of Chemical Physics*, **137**, Article ID: 214311. https://doi.org/10.1063/1.4769282

[26] Yang, W.J., Gao, Z.Y., Liu, X.S., Li, X., Ding, X.L. and Yan, W.P. (2018) Single-Atom Iron Catalyst with Single-Vacancy Graphene-Based Substrate as a Novel Catalyst for NO Oxidation: A Theoretical Study. *Catalysis Science & Technology*, **8**, 4159-4168. https://doi.org/10.1039/C8CY01225C

[27] Wang, Y.Y., Deng, J.J., Wang, X., Che, J.T. and Ding, X.L. (2018) Small Stoichiometric $(MoS_2)_n$ Clusters with the 1T Phase. *Physical Chemistry Chemical Physics*, **20**, 6365-6373. https://doi.org/10.1039/C7CP07914A

[28] Ding, X.L., Wang, D., Li, R.J., Liao, H.L., Zhang, Y. and Zhang, H.Y. (2016) Adsorption of a Single Gold or Silver Atom on Vanadium Oxide Clusters. *Physical Chemistry Chemical Physics*, **18**, 9497-9503. https://doi.org/10.1039/C6CP00808A

[29] Ding, X.L., Liao, H.L., Zhang, Y., Chen, Y.M., Wang, D., Wang, Y.Y. and Zhang, H.Y. (2016) Geometric and Electronic Properties of Gold Clusters Doped with a Single Oxygen Atom. *Physical Chemistry Chemical Physics*, **18**, 28960-28972. https://doi.org/10.1039/C6CP05595H

[30] Ding, X.L., Wang, D., Wu, X.N., Li, Z.Y., Zhao, Y.X. and He, S.G. (2015) High Reactivity of Nanosized Niobium Oxide Cluster Cations in Methane Activation: A Comparison with Vanadium Oxides. *The Journal of Chemical Physics*, **143**, Article ID: 124312. https://doi.org/10.1063/1.4931972

[31] Chen, Y., Deng, J.J., Yao, W.W., Gurti, J.I., Li, W., Wang, W.J., Yao, J.X. and Ding, X.L. (2021) Non-Stoichiometric Molybdenum Sulfide Clusters and Their Reactions with the Hydrogen Molecule. *Physical Chemistry Chemical Physics*, **23**, 347-355. https://doi.org/10.1039/D0CP04457A

[32] Schäfer, A., Huber, C. and Ahlrichs, R. (1994) Fully Optimized Contracted Gaussian Basis Sets of Triple Zeta Valence Quality for Atoms Li to Kr. *The Journal of Chemical Physics*, **100**, 5829-5835. https://doi.org/10.1063/1.467146

[33] Dolg, M., Stoll, H. and Preuss, H. (1989) Energy-Adjusted *Ab initio* Pseudopotentials for the Rare Earth Elements. *The Journal of Chemical Physics*, **90**, 1730-1734. https://doi.org/10.1063/1.456066

[34] Papajak, E., Zheng, J.J., Xu, X.F., Leverentz, H.R. and Truhlar, D.G. (2011) Perspectives on Basis Sets Beautiful: Seasonal Plantings of Diffuse Basis Functions. *Journal*

of Chemical Theory and Computation, **7**, 3027-3034.
https://doi.org/10.1021/ct200106a

[35] Zheng, J.J., Xu, X.F. and Truhlar, D.G. (2011) Minimally Augmented Karlsruhe Basis Sets. *Theoretical Chemistry Accounts*, **128**, 295-305.
https://doi.org/10.1007/s00214-010-0846-z

[36] Tao, J., Perdew, J.P., Staroverov, V.N. and Scuseria, G.E. (2003) Climbing the Density Functional Ladder: Non-Empirical Meta-Generalized Gradient Approximation Designed for Molecules and Solids. *Physical Review Letters*, **91**, Article ID: 146401.
https://doi.org/10.1103/PhysRevLett.91.146401

[37] Lu, T. (2020) sobMECP Program. http://sobereva.com/286 (Accessed Nov 6, 2020)

[38] Lu, T. and Chen, F.W. (2012) Multiwfn: A Multifunctional Wavefunction Analyzer. *Journal of Computational Chemistry*, **33**, 580-592. https://doi.org/10.1002/jcc.22885

[39] Zhang, H.-X. and Ding, X.-L. (2016) DFT Investigations on $AuVO_3^+$, a Barrier-Free Catalyst for Oxidation of CO with O_2. *Chemical Physics*, **475**, 69-76.
https://doi.org/10.1016/j.chemphys.2016.06.009